

# Lowest Excitations in $^{56}\text{Ti}$ and the Predicted $N = 34$ Shell Closure

S.N. Liddick<sup>1,2</sup>, P.F. Mantica<sup>1,2</sup>, R.V.F. Janssens<sup>3</sup>, R. Broda<sup>4</sup>, B.A. Brown<sup>1,5</sup>,  
M.P. Carpenter<sup>3</sup>, B. Fornal<sup>4</sup>, M. Honma<sup>6</sup>, T. Mizusaki<sup>7</sup>, A.C. Morton<sup>1</sup>, W.F. Mueller<sup>1</sup>,  
T. Otsuka<sup>8</sup>, J. Pavan<sup>9</sup>, A. Stolz<sup>1</sup>, S.L. Tabor<sup>9</sup>, B.E. Tomlin<sup>1,2</sup>, M. Wiedeking<sup>9</sup>

<sup>(1)</sup> *National Superconducting Cyclotron Laboratory,*

*Michigan State University, East Lansing, Michigan 48824*

<sup>(2)</sup> *Department of Chemistry, Michigan State University, East Lansing, Michigan 48824*

<sup>(3)</sup> *Physics Division, Argonne National Laboratory, Argonne, Illinois 60439*

<sup>(4)</sup> *Niewodniczanski Institute of Nuclear Physics, PL-31342 Cracow, Poland*

<sup>(5)</sup> *Department of Physics and Astronomy,*

*Michigan State University, East Lansing, Michigan 48824*

<sup>(6)</sup> *Center for Mathematical Sciences,*

*University of Aizu, Tsuruga, Ikki-machi,*

*Aizu-Wakamatsu, Fukushima 965-8580, Japan*

<sup>(7)</sup> *Institute of Natural Sciences, Senshu University,*

*Higashimita, Tama, Kawasaki, Kanagawa 214-8580, Japan*

<sup>(8)</sup> *Department of Physics, University of Tokyo,*

*Hongo, Tokyo 113-0033, Japan and RIKEN,*

*Hirosawa, Wako-shi, Saitama 351-0198, Japan and*

<sup>(9)</sup> *Department of Physics, Florida State University, Tallahassee, Florida 32306*

(Dated: January 6, 2004)

## Abstract

Recent experimental characterization of the subshell closure at  $N = 32$  in the Ca, Ti, and Cr isotones has stimulated shell-model calculations that indicated the possibility that the  $N = 34$  isotones of these same elements could exhibit characteristics of a shell closure, namely a high energy for the first excited  $2^+$  level. To that end, we have studied the decay of  $^{56}\text{Sc}$  produced in fragmentation reactions and identified new  $\gamma$  rays in the daughter  $N = 34$  isotone  $^{56}\text{Ti}$ . The first  $2^+$  level is found at an energy of 1127 keV, well below the expected position that would indicate the presence of an  $N = 34$  shell closure in  $^{56}\text{Ti}$ .

The inclusion of a spin-orbit force into the nuclear shell model by Mayer and Jensen [1, 2] enabled the reproduction of the known magic numbers near stability. As a result, the shell model became a powerful predictive tool. However, recent advances in rare isotope beams have greatly increased the number of exotic nuclei that are available for study and there are indications that the extrapolation of the shell model to these new regions is not straightforward. As exotic nuclei are studied, unforeseen modifications to shell structure have been encountered and it is possible that the traditional magic numbers, on which the shell model rests, may not extend far from the valley of stability, especially in neutron-rich systems. The development of a diffuse neutron surface may result in a diminished spin-orbit interaction, washing out some energy gaps between major neutron shells, and creating others [3, 4]. Additionally, a proton-neutron monopole interaction could be responsible for a reordering of single-particle orbits and the development of new shell closures.

The effects of a strong proton-neutron monopole interaction on the location of single-particle states have been observed close to stability in the  $N = 50 - 82$  major shell. A strongly attractive monopole proton-neutron interaction, whose strength is maximized when  $\ell(\text{proton}) \sim \ell(\text{neutron})$  [5], is believed to be responsible for a shift in the  $\nu 1g_{7/2}$  single-particle energy. The filling of the  $\pi 1g_{9/2}$  orbital results in a lowering of the  $\nu 1g_{7/2}$  state by approximately 3 MeV relative to the  $\nu 2d_{3/2}$  orbit between  $^{91}\text{Zr}_{51}$  and  $^{131}\text{Sn}_{81}$  [6]. Although the single-particle level density is high in this mass region, the drastic change in the single-particle energies results in the formation of a shell gap at  $N = 56$ , evidenced by the high  $2_1^+$  energy in  $^{96}\text{Zr}$  [7] compared to other Zr isotopes that subsequently is washed out as  $Z$  increases.

In regions of low single-particle level density, such as the *sd* and *pf* shells, the substantial reordering of single-particle states due to the proton-neutron monopole interaction makes neutron-rich nuclei near  $N = 20$  and  $N = 28$  ideal candidates for the emergence of new shell closures. The erosion of the  $N = 20$  shell gap, leading to the development of the  $N = 16$  shell closure [8] has been attributed to a proton-neutron monopole interaction between spin-orbit partners in the *sd* shell, in this case the  $\pi 1d_{5/2}$  and  $\nu 1d_{3/2}$  orbits [4]. As protons are removed from the  $\pi 1d_{5/2}$  orbit, the neutron  $\nu 1d_{3/2}$  state rises in energy until it nears the *pf* shell, eroding the  $N = 20$  gap.

In the *pf* shell, a  $\pi 1f_{7/2} - \nu 1f_{5/2}$  monopole interaction is responsible for a nearly 3 MeV shift in the energy of the  $\nu 1f_{5/2}$  state, relative to the  $\nu 1p_{3/2}$  level, between the  $N = 29$

isotones  $^{49}\text{Ca}$  and  $^{57}\text{Ni}$  as protons are added to the  $\pi 1f_{7/2}$  orbital. Though similar in magnitude to the shift observed in the  $N = 50 - 82$  major shell, the monopole interaction has a substantial effect on the development of new shell gaps due to the relatively low density of single-particle states. The migration of the  $\nu 1f_{5/2}$  orbital to higher energies with the removal of protons from the  $1f_{7/2}$  orbital, in combination with the large spin-orbit splitting observed for  $\nu 2p_{3/2} - \nu 2p_{1/2}$ , has been invoked [9] to account for the appearance of an  $N = 32$  subshell closure for neutron-rich nuclides, which has been demonstrated experimentally for the neutron-rich nuclides  $^{56}_{24}\text{Cr}$ ,  $^{54}_{22}\text{Ti}$ , and  $^{52}_{20}\text{Ca}$  [9–13].

Recently, a new effective interaction, labelled GXPF1, for use in the full  $pf$ -shell was proposed by Honma *et al.* [14]. Shell model calculations with this interaction reproduce well the systematic variation in the energy of the first excited  $2^+$  states [ $E(2^+_1)$ ] for the Cr nuclides around  $N = 32$  [10], as well as that of the high-spin states in the even-even Ti isotopes [11], both strong indicators of a significant subshell gap at  $N = 32$ . An intriguing result of these calculations is the expectation that a sizable energy gap should occur in the effective neutron single-particle energies between the  $\nu 2p_{1/2}$  and  $\nu 1f_{5/2}$  orbitals leading to the development of  $N = 34$  as a new magic number for neutron-rich nuclides with  $Z \leq 22$  [4].

The goal of the study reported herein was to determine  $E(2^+_1)$  in  $^{56}\text{Ti}_{34}$  in order to provide experimental evidence for the presence of the proposed shell closure at  $N = 34$ . The parent nuclide  $^{56}\text{Sc}$ , along with several other neutron-rich nuclei, was produced using the facilities at the National Superconducting Cyclotron Laboratory (NSCL). A primary beam of  $^{86}\text{Kr}$  was accelerated to 140 MeV/nucleon using the coupled K500 and K1200 cyclotrons and fragmented in a  $343 \text{ mg/cm}^2$   $^9\text{Be}$  target placed at the object position of the A1900 fragment separator [15]. The desired isotopes were separated in the A1900 and implanted into a  $4 \text{ cm} \times 4 \text{ cm} \times 1500 \text{ }\mu\text{m}$  double-sided Si strip detector (DSSD), segmented into 40 1-mm strips in the x and y dimensions. Particle identification was derived from energy loss and fragment time of flight (relative to the cyclotron frequency) from a  $474 \text{ }\mu\text{m}$  PIN detector (PIN1) located approximately 1 m upstream of the DSSD. The DSSD was placed between a  $966 \text{ }\mu\text{m}$  PIN detector (upstream) and the NSCL  $\beta$  calorimeter [16] (downstream). A 5 cm thick plastic scintillator was placed downstream of the calorimeter to detect light particles transmitted with the desired fragments. The hardware trigger used in the data acquisition required a front and back signal in the DSSD in anti-coincidence with the scintillator, which

reduced the number of events recorded due to unwanted light particles. The incoming beam was defocused to illuminate  $\approx 2/3$  of the DSSD resulting in an average time of 90 seconds between successive implants in a given pixel near the center of the DSSD.  $\beta$ -delayed  $\gamma$  rays were monitored using twelve HPGe detectors from the MSU Segmented Germanium Array (SeGA)[17]. An efficiency of 5.3% at 1 MeV was deduced for the array in this configuration.

Data were written event-by-event using the trigger conditions described above. Each event was time stamped by a free running clock having a resolution of 30.5  $\mu$ s. Fragment- $\beta$  coincidences were established in software based on the correlation of valid implants and decays for those signals that were above a predetermined threshold (approximately 110 keV for decay events). The performance of the DSSD when correlating implants and decays in the same pixel is described in Ref. [18]. For the present study, the implantation rate was low enough ( $<10$  Hz) to allow an expanded correlation. Decays were correlated with either an implant in the same pixel or one of the eight surrounding pixels. To reduce background, both the maximum correlation time and the minimum time between successive implants were set to one second. In this manner the efficiency for correlating  $\beta$  decays with  $^{56}\text{Sc}$  implants was 40%. Additional experimental details can be found in Ref. [10, 11, 19].

The  $\beta$ -delayed  $\gamma$ -ray spectrum for events that occurred within one second after a  $^{56}\text{Sc}$  implant is shown in Fig. 1. Seven transitions have been identified in the spectrum. Two  $\gamma$  rays located at  $666\pm 1$  and  $1005\pm 1$  keV are attributed to known transitions in  $^{56}\text{Cr}$  [10]. The 666-keV transition falls outside  $1\sigma$  from the energy reported in Ref. [10], and may be a transition in  $^{56}\text{Ti}$ . As there are no  $\gamma$ -rays assigned following the  $\beta$  decay of  $^{56}\text{Sc}$  [19], the five remaining transitions, listed with their absolute intensities, are assigned to the decay of  $^{56}\text{Sc}$ :  $592\pm 1$  keV ( $7\pm 2\%$ ),  $689\pm 1$  keV ( $19\pm 4\%$ ),  $751\pm 1$  keV ( $9\pm 3\%$ ),  $1127\pm 1$  keV ( $48\pm 11\%$ ), and  $1160\pm 1$  keV ( $21\pm 5\%$ ). The 1127-keV transition is the most intense and is proposed as the  $2^+ \rightarrow 0^+$  transition in  $^{56}\text{Ti}$ . The 1127- and 689-keV  $\gamma$  rays are in coincidence, as determined by gating on the two transitions in a  $\gamma$ - $\gamma$  coincidence matrix. The lack of statistics in this matrix for the other three transitions makes it difficult to establish their location in the decay scheme presented in Fig. 2.

The absolute intensities of the observed  $\gamma$  rays were calculated from the  $\beta$ - $\gamma$  spectrum, the SeGA efficiency, and the total number of  $^{56}\text{Sc}$  decays obtained from the half-life curve. If all transitions pass through the 1127-keV energy level, an upper limit of 52% is established for ground state feeding. This branch could be reduced if any of the unassigned  $\gamma$  rays

directly feed the ground state of  $^{56}\text{Ti}$ , however, such a scenario would result in at least one excited level either below the 1127-keV state or, in the case of the 1160-keV transition, only 33-keV above the proposed  $2_1^+$  state. More likely, these unplaced  $\gamma$  rays populate higher energy states in  $^{56}\text{Ti}$ .  $\text{Log}ft$  values were calculated for the different  $\beta$  branches using  $Q_\beta = 13700 \pm 800$  keV obtained from Ref. [20] and a half-life of  $38 \pm 5$  ms extracted from the decay curve of  $^{56}\text{Sc}$ . A  $\text{log}ft$  value of 4.8 was determined for direct feeding to the ground state and suggests an allowed transition. Therefore, we have tentatively assigned a spin and parity of  $1^+$  to the ground state of the  $^{56}\text{Sc}$  parent. Unobserved decays with intensities below our detection threshold of  $\sim 6\%$  or new coincidence data could change the  $\text{log}ft$  values and current results should be treated as lower limits.

Shell model calculations [21] have been performed using the GXPF1 [14] and KB3G [22] interactions in an attempt to describe the migration of the  $\nu 1f_{5/2}$  single-particle orbit, due to the monopole interaction, as protons are removed from the  $\pi 1f_{7/2}$  shell. The results of these calculations and recent experimental data on the systematics of the  $E(2_1^+)$  for the Ti and Ca isotopes are compared in Fig. 3. The GXPF1 calculations predict a large separation between the  $\nu 1f_{5/2}$  and  $\nu 2p_{3/2}$  single-particle orbits for nuclei with  $Z \leq 24$ . The energy gap between these two orbitals, combined with a low single-particle level density in this region, gives rise to the development of a subshell closure at  $N = 32$ . This closure is manifested in the increased energy of the  $2_1^+$  levels for Cr, Ti, and Ca and this rise in  $E(2_1^+)$  has been verified experimentally [9–13]. GXPF1 also predicts that a large energy separation between the  $\nu 2p_{1/2}$  and  $\nu 1f_{5/2}$  orbitals develops for nuclei with  $Z \leq 22$ . In fact, the energy separation between the two orbitals is calculated to be large enough to give rise to a shell closure at  $N = 34$  for Ti and Ca. The KB3G calculations do not predict a shell closure at  $N = 34$ . The first evidence for this shell closure should be manifested in an increased  $E(2_1^+)$ , predicted at an energy of 1509 keV in  $^{56}\text{Ti}$  [11, 14]. This energy is very close to the 1495 keV energy established experimentally for the  $2_1^+$  level in  $^{54}\text{Ti}$ , attributed to the  $N = 32$  subshell closure. However, an energy of 1127 keV is observed for the  $2_1^+$  state in  $^{56}\text{Ti}$ , almost 400 keV lower than predicted (Fig. 3) using GXPF1, but can be explained if the  $\nu 1f_{5/2}$  orbital is lower by  $\sim 0.8$  MeV. To preserve the calculated energies of the  $\nu 1f_{5/2}$  level in higher- $Z$  nuclei a weaker monopole interaction between the  $\pi 1f_{7/2}$  and  $\nu 1f_{5/2}$  states is also indicated. With the decrease of the  $\nu 1f_{5/2}$  state by 0.8 MeV, the  $N = 34$  shell gap at  $^{54}\text{Ca}$  is still a little greater than 3 MeV. Thus, the presently observed  $2_1^+$  energy is consistent with the prediction

of an  $N = 34$  shell gap but requires some small alterations in the GXPF1 interaction.

From the ground-state  $\beta$ -decay branching ratios and  $\log ft$  values for the neighboring odd-odd nuclei, the monopole migration of the  $\nu 1f_{5/2}$  state with the removal of  $\pi 1f_{7/2}$  protons can be followed. The spin and parity of both  $^{56,58}\text{V}$  were assigned as  $1^+$  [10] due to the presence of  $\beta$ -decay observables consistent with allowed transitions. In an extreme single-particle model, assuming  $N = 32$  is a good subshell, the spins and parities of the  $^{56,58}\text{V}$  ground states result from the coupling of the odd valence proton and neutron. The  $_{23}\text{V}$  isotopes contain an odd proton in the  $\pi 1f_{7/2}$  orbit. Coupling to a neutron in the  $\nu 1f_{5/2}$  orbit results in spins and parity  $(1-6)^+$ . The ground states of  $^{56,58}\text{V}$  are both  $1^+$ , suggesting that the  $33^{rd}$  and  $35^{th}$  neutrons fill the  $\nu 1f_{5/2}$  orbit. Combined with the observed increase in the value of the  $E(2_1^+)$ , compared to neighboring isotopes, the  $\nu 1f_{5/2}$  orbit seems to have risen in energy to just below the  $\nu 2p_{1/2}$  level, producing an energy gap between the  $\nu 1f_{5/2}$  and  $\nu 2p_{3/2}$  states and a subshell closure at  $N = 32$ . The presence of an  $N = 32$  subshell closure is further bolstered by the systematic studies of high-spin states in  $^{50-54}\text{Ti}$  [11].

For  $^{54,56}\text{Sc}$ , the ground state spin and parity have been tentatively assigned as  $3^+$  [11] and  $1^+$ , respectively, based on the  $\beta$  decay feeding pattern. Using the same single-particle picture as above, the odd proton in  $_{21}\text{Sc}$  is located in the  $\pi 1f_{7/2}$  orbit and will couple to the odd neutron in  $^{54,56}\text{Sc}$ . The  $3^+$  ground state for  $^{54}\text{Sc}$  indicates that the  $33^{rd}$  neutron may occupy the  $\nu 2p_{1/2}$  orbit. Though it is possible to obtain a  $3^+$  ground state with a neutron in the  $\nu 1f_{5/2}$  state, Nordheim rules [23, 24] argue against it. In  $^{56}\text{Sc}$ , the ground state becomes  $1^+$  as expected if the  $35^{th}$  neutron begins to fill the  $\nu 1f_{5/2}$  orbital. Therefore, the  $\nu 1f_{5/2}$  level continues to migrate towards higher energies in the  $_{21}\text{Sc}$  isotopes and seems to be located above the  $\nu 2p_{1/2}$  orbit.

Thus, from the spin and parities of the ground states in the odd-odd Sc and V isotopes, the migration of the  $\nu 1f_{5/2}$  single-particle orbital appears to follow the general trend predicted by shell-model calculations. The single-particle energy of the  $\nu 1f_{5/2}$  orbital increases in energy leading to an inversion of the  $\nu 1f_{5/2}$  and  $\nu 1p_{1/2}$  level ordering between V and Sc. While the ordering of the levels agrees with calculations, the  $E(2_1^+)$  measurement suggests that the degree of separation between the  $\nu 2p_{1/2}$  and  $\nu 1f_{5/2}$  states is not sufficient to produce the anticipated shell closure at  $N = 34$  in Ti.

The absence of the  $N = 34$  shell closure at  $^{56}\text{Ti}$  could be attributed the reduction of the  $\nu 1f_{5/2}$  state by  $\sim 0.8$  MeV and a weaker monopole interaction, resulting in a decreased

energy gap between the  $\nu 1f_{5/2}$  and  $\nu 2p_{1/2}$  levels for Ti nuclides, inhibiting the formation of a  $N = 34$  shell closure. This does not mean, however, that the  $N = 34$  shell closure may not be present in  $^{54}\text{Ca}$ : the lack of protons in the  $\pi 1f_{7/2}$  orbit in the  $^{20}\text{Ca}$  isotopes could still lead to a large separation between the  $\nu 1f_{5/2}$  and  $\nu 2p_{1/2}$  states and produce a shell closure at  $N = 34$ .

In summary, the  $\beta$  decay of  $^{56}\text{Sc}$  was used to populate the low-energy level structure of  $^{56}\text{Ti}$ . A  $\beta$ -delayed  $\gamma$  ray has been observed at 1127 keV and assigned to the  $2^+ \rightarrow 0^+$  transition in  $^{56}\text{Ti}$ , midway between GXPF1 and KB3G predictions. The systematic variation of the  $E(2_1^+)$  values for the neutron-rich Ti isotopes does not show evidence for a significant shell closure at  $N = 34$ , in disagreement with the predictions of shell model calculations using the GXPF1 interaction. A lowering of the  $\nu 1f_{5/2}$  single-particle energy with a weaker monopole interaction would bring the  $\nu 1f_{5/2}$  and  $\nu 2p_{1/2}$  orbits closer in energy and retard the formation of a  $N = 34$  shell closure for Ti nuclides. A significant shell closure at  $N = 34$  may still be present for Ca. The continued monopole shift of the  $\nu 1f_{5/2}$  orbital with the removal of the last two protons from the  $\pi 1f_{7/2}$  shell may result in a significant gap in the effective single-particle energies between the  $\nu 1p_{1/2}$  and  $\nu 1f_{5/2}$  states. Future experiments on the neutron-rich Ca isotopes are warranted to track this progression.

This work was supported in part by the National Science Foundation Grant Nos. PHY-01-10253, PHY-97-24299, PHY-01-39950, PHY-0244453, and PHY-00-70911, the U.S. Department of Energy, Nuclear Physics Division, under Contract No. W31-109-ENG-38, and the Polish Scientific Committee Grant No. 2P03B-074-1. The authors would like to thank the NSCL operations staff for their support in conducting this experiment.

- 
- [1] M. G. Mayer, *Phys. Rev.* **75**, 1969 (1949).
  - [2] O. Haxel *et al.*, *Phys. Rev.* **75**, 1776 (1949).
  - [3] J. Dobaczewski *et al.*, *Phys. Rev. Lett.* **72**, 981 (1994).
  - [4] T. Otsuka *et al.*, *Phys. Rev. Lett.* **87**, 082502 (2001).
  - [5] P. Federman and S. Pittel, *Phys. Lett.* **69B**, 385 (1977).
  - [6] R. A. Meyer *et al.*, *Exotic Nuclear Spectroscopy*, ed., (Plenum Press, New York, 1990).
  - [7] *Table of Isotopes*, 8th edition, R.B. Firestone, ed., (Wiley, New York, 1996).



- [8] A. Ozawa *et al.*, Phys. Rev. Lett. **84**, 5493 (2000).
- [9] J. I. Prisciandaro *et al.*, Phys. Lett. B **510**, 17 (2001).
- [10] P. F. Mantica *et al.*, Phys. Rev. C **67**, 014311 (2003).
- [11] R. V. F. Janssens *et al.*, Phys. Lett. B **546**, 55 (2002).
- [12] D. E. Appelbe *et al.*, Phys. Rev. C **67**, 034309 (2003).
- [13] A. Huck *et al.*, Phys. Rev. C **31**, 2226 (1985)
- [14] M. Honma *et al.*, Phys. Rev. C **65**, 061301 (2002).
- [15] D. J. Morrissey *et al.*, Nucl. Instrum. Methods Phys. Res. B **204**, 90 (2003).
- [16] A. C. Morton, AIP Conference Proceedings, **680**, 550 (2003).
- [17] W. F. Mueller *et al.*, Nucl. Instrum. Methods Phys. Res. **A466**, 492 (2001).
- [18] J. I. Prisciandaro *et al.*, Nucl. Instrum. Methods Phys. Res. **A505**, 140 (2003).
- [19] P. F. Mantica *et al.*, Phys. Rev. C **68**, 044311 (2003).
- [20] G. Audi and A. H. Wapstra, Nucl. Phys. **A595**, 409 (1995).
- [21] T. Mizusaki, computer code MSHELL, RIKEN Accel. Prog. Rep. **33**, 14 (2000).
- [22] A. Poves *et al.*, Nucl. Phys. **A694**, 157, (2001)
- [23] L. Nordheim, Rev. Mod. Phys. **23**, 322 (1951).
- [24] M.H. Brennan and A.M. Bernstein, Phys. Rev. **120**, 927 (1960).

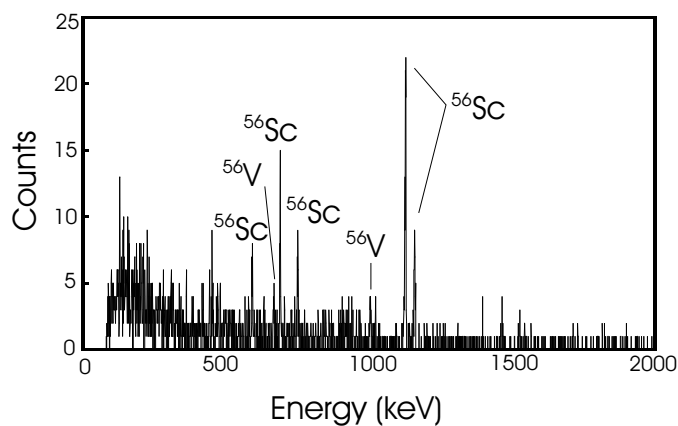


FIG. 1: Part of the  $\beta$ -delayed  $\gamma$ -ray spectrum in the range 0 - 2000 keV for events occurring within the first second after a  $^{56}\text{Sc}$  implant.

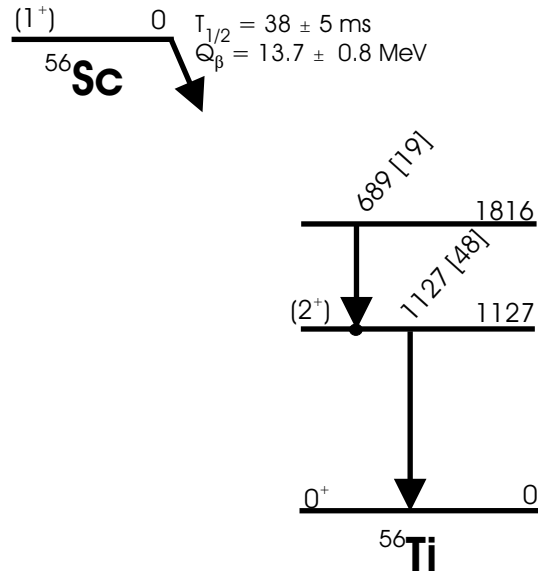


FIG. 2: Proposed level scheme for  $^{56}\text{Ti}$ . The absolute intensity of a  $\gamma$  ray is shown in brackets following the  $\gamma$ -ray decay energy. The  $Q_\beta$  value was determined from mass excess data [20]. The filled circle represents known coincidences.

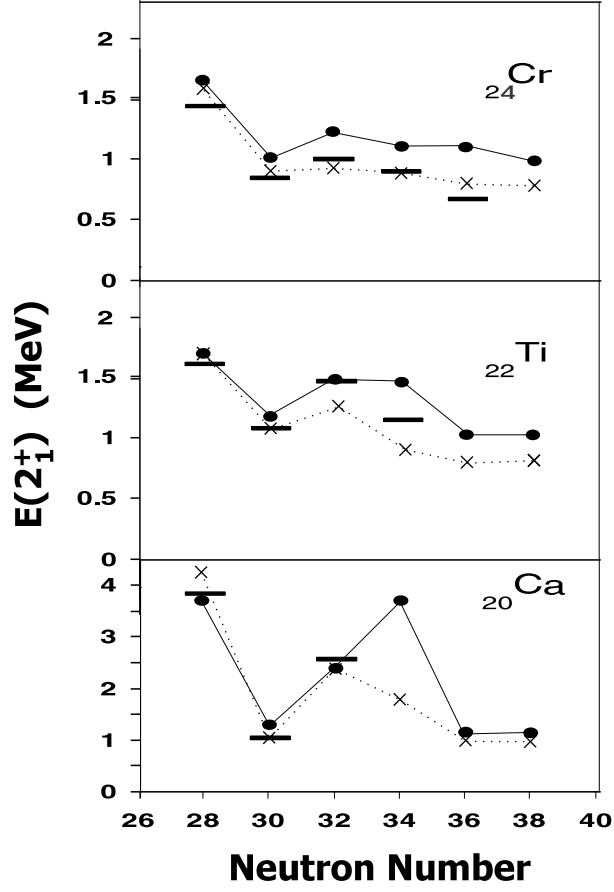


FIG. 3:  $E(2_1^+)$  values versus neutron number for the even-even  $^{24}\text{Cr}$ ,  $^{22}\text{Ti}$ , and  $^{20}\text{Ca}$  isotopes. Experimental values are denoted by dashes. Shell model calculations using the GXPF1 [14] and KB3G [22] interactions are shown as filled circles and crosses, respectively.